1999

SiC and Si_3N_4 recession due to SiO_2 scale volatility under combustor conditions

James L. Smialek
NASA Glenn Research Center, james.l.smialek@nasa.gov

R. Craig Robinson
NASA Glenn Research Center

Elizabeth J. Opila
NASA Glenn Research Center

Dennis S. Fox
NASA Glenn Research Center

Nathan S. Jacobson
NASA Glenn Research Center

Adv. Composite Mater., Vol. 8, No. 1, pp. 33–45 (1999)

SiC and Si_3N_4 recession due to SiO_2 scale volatility under combustor conditions *

JAMES L. SMIALEK †, R. CRAIG ROBINSON, ELIZABETH J. OPILA, DENNIS S. FOX and NATHAN S. JACOBSON

NASA Lewis Research Center, 21000 Brookpark Road, Cleveland OH 44135, USA

Abstract—SiC and Si_3N_4 materials were tested under various turbine engine combustion environments, chosen to represent either conventional fuel-lean or fuel-rich mixtures proposed for high speed aircraft. Representative CVD, sintered, and composite materials were evaluated in both furnace and high pressure burner rig exposure. While protective SiO_2 scales form in all cases, evidence is presented to support paralinear growth kinetics, i.e. parabolic growth moderated simultaneously by linear volatilization. The volatility rate is dependent on temperature, moisture content, system pressure, and gas velocity. The burner tests were used to map SiO_2 volatility (and SiC recession) over a range of temperature, pressure, and velocity. The functional dependency of material recession (volatility) that emerged followed the form: $\exp(-Q/RT) * P^x * v^y$. These empirical relations were compared to rates predicted from the thermodynamics of volatile SiO and SiO_xH_y reaction products and a kinetic model of diffusion through a moving boundary layer. For typical combustion conditions, recession of 0.2 to 2 μm/h is predicted at 1200–1400°C, far in excess of acceptable long term limits.

Keywords: SiC; Si_3N_4; oxidation; scale volatility; combustor; water vapor.

1. INTRODUCTION

SiC composites have been proposed as liner material for advanced combustors in turbine engines. Operational pressures are in the vicinity of about 10 atm. Conventional (lean) operation produces a combustion product consisting of $10\%O_2-8\%H_2O-7\%CO_2-$bal. N_2 at an equivalence ratio, ϕ, of 0.5 [1]. Other combustor concepts use a rich-burn pre-chamber in which a hypostoichiometric mixture of fuel-to-air (ϕ of about 1.5) is burned. A $6\%H_2-12\%H_2O-12\%CO-5\%CO_2-$bal. N_2 combustion chemistry is projected here. The rich-burn segment is followed by

*Prepared for Processing and Testing on CMC Parts, Components and Pieces, The Satellite Workshop of the HT-CMC3 Conference, September 11–12, 1998, Tajimi-City, Gifu, Japan.

†E-mail: James.L.Smialek@LeRC.NASA.gov

a quick air-quench and lean aft-burn segment. Volatile reaction products between the SiO_2 scales and the combustion gases have been a concern on this program. It was shown that the allied furnace TGA exposures produce $Si(OH)_4$ (g) and SiO (g), respectively, when SiC is exposed to model lean and rich gases [2–4]. Although a scale is first produced by oxidation, it then reacts with the gas to form a volatile secondary product. This gives rise to paralinear kinetics and accelerated consumption of the substrate (recession) [2]. This represents a non-protective oxidation regime, and long term exposures produce linear attack rates. These rates are determined by the thermodynamics of the equilibrium vapor species, the ambient pressure, and the gas velocity. While a number of burner rig studies have been performed on SiC [5], only one has recently combined the use of high pressure and high velocity and clearly produced weight loss [6]. No previous studies have addressed the effect of rich-burn combustion.

Thus the purpose of this study was to examine the behavior of pure CVD SiC under a variety of high temperature, pressure, and velocity conditions in both lean-burn and rich-burn combustion environments. This was accomplished in a high pressure burner rig (HPBR). Some experimental results are covered in more detail in previous reports [7, 8], and chemical mechanisms are covered in greater depth in [9]. The volatility rates in HPBR tests are compared to those measured in the furnace TGA tests and those calculated from the thermodynamic diffusion model. Recession rates were also obtained on CVD and sintered Si_3N_4 material for comparison.

2. EXPERIMENTAL

High purity CVD SiC and Si_3N_4 materials (Bomas Machine Specialties and Advanced Ceramics Corp.) were machined to $0.3 \times 1.3 \times 2.5$ cm TGA specimens or $0.3 \times 1.3 \times 7.6$ cm HPBR specimens. TGA tests were performed with Cahn 1000 microbalances and furnaces using quartz tubes. Model lean exposures employed a $50\%H_2O/O_2$ mixture to approach the high water vapor pressure of a combustor environment [2]. (A moisture content of $8\% \times 10$ atm, or 80%, would be more representative of the actual combustor conditions.) A special double-chamber water saturator, followed by tape-heated gas lines, was employed to insure accurate control of the moisture content. The gas flow was 4.4 cm/s. Model rich exposures were made in a premixed gas flowing through a similar saturator to give $4\%H_2-12\%H_2O-10\%CO-7\%CO_2-N_2$, flowing at 0.44 cm/s [4].

An existing high pressure burner rig was extensively modified to allow both lean and rich-burn testing of multiple ceramic specimens (Fig. 1). Details of the construction and operation can be found in [7, 8]. The basic operation entails pressurized fuel and air injection (in an air blast nozzle and swirl plate dome section), ignition (by hydrogen gas at a spark plug), and combustion product formation (in an air-cooled, TBC-coated combustor can). The gaseous combustion products proceed through a water-cooled transition section, losing heat in the process. Specimens

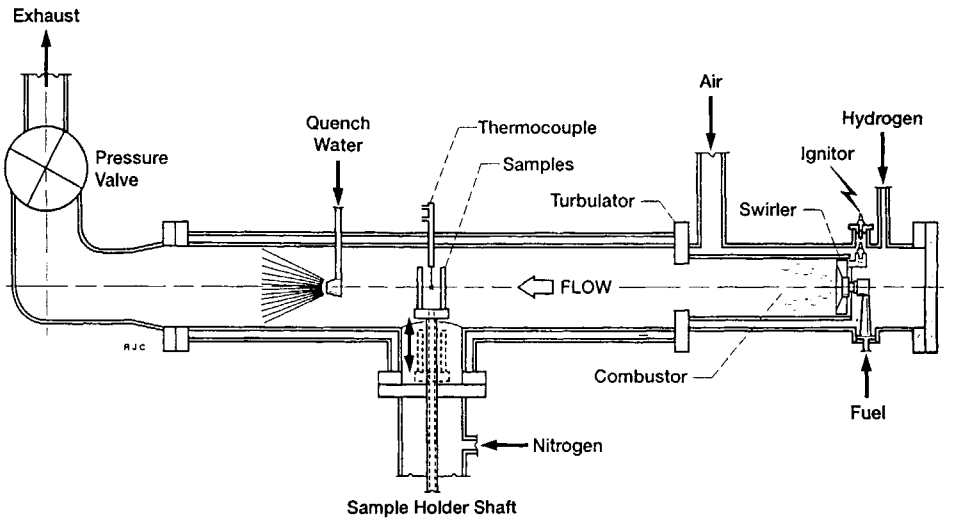

Figure 1. Schematic diagram of NASA Lewis High Pressure Burner Rig.

are arranged in a wedge configuration in a water-cooled specimen holder, pneumatically actuated into or out of the flowing gas. Gas temperature is measured by a Pt–Pt13Rh thermocouple at a position just behind the samples. Sample temperature was measured by two-color optical and laser pyrometry (lean-burn only). Rich-burn temperatures were determined from a thermocouple measurement of gas temperature and specimen temperature calibration curve, as determined in the lean mode. This was necessary because the luminous flame in rich operation precluded measurements by optical pyrometry.

It was intended to determine volatility rates over a range of temperature, pressure, and velocity. To this end, some flexibility in operational parameters exists; however, an interdependence between variables resulted in certain restrictions. Nominal fuel-lean combustion at $\phi = 0.8–0.9$ and fuel-rich at $\phi = 1.8–2.0$ produced sample temperatures from 1200–1450°C. Standard operating pressure and velocity was 6 atm and 18–25 m/s, respectively. For a select number of tests, pressure was also varied from 4–15 atm, while velocity for the most part was a dependent variable.

3. RESULTS

3.1. Furnace tests

In model lean furnace tests, mixtures of $10\%H_2O/O_2$ failed to produce appreciable differences in kinetics from those performed in dry O_2 environments. However, at $50\%H_2O/O_2$, which would be more representative of a moist environment at high pressures, a negative (paralinear) deviation from parabolic kinetics was observed. Analysis of weight change data yields both a parabolic growth constant, k_p, and a linear recession rate, k_l [2]. A typical curve and fitted parameters for CVD SiC

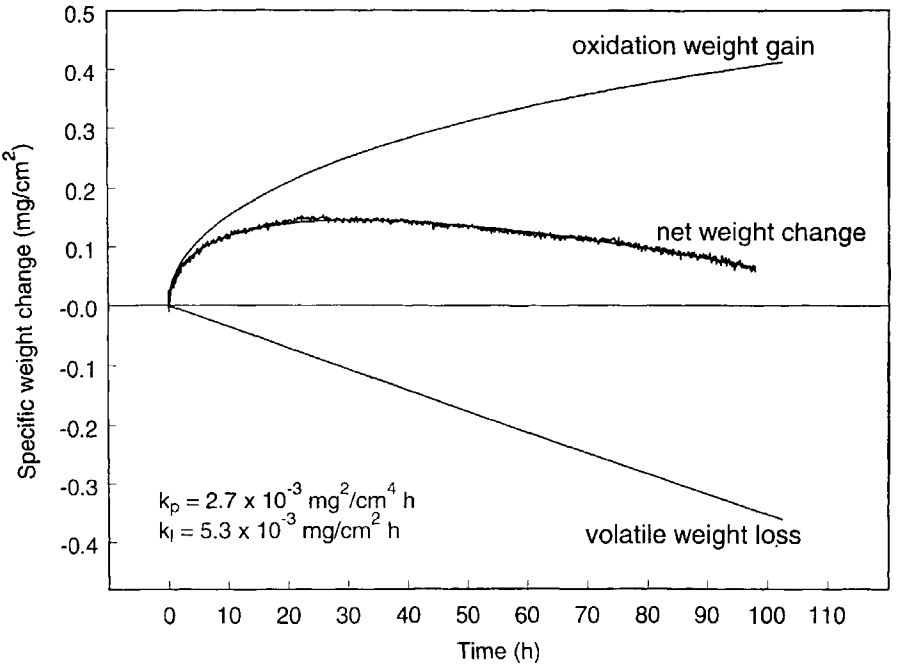

Figure 2. Paralinear weight change curves for CVD SiC in synthetic lean 50%H_2O/O_2 furnace TGA environment at 1200°C. The model curves indicate the amount of oxygen gain in the scale present, the amount of silicon (and carbon) lost due to scale volatility, and the net weight change.

oxidized in 50%H_2O/O_2 (lean) at 1200°C is given in Fig. 2. The actual (sawtooth) data and fitted 'net weight change' (smooth) curves are coincident and provide a high degree of confidence for the mathematical model. The model 'weight gain' curve is indicative of the amount of scale present on the sample, while the model 'weight loss' curve indicates the amount of Si (and C) lost during oxidation and SiO_2 scale volatilization. There was only a slight temperature dependence of k_p and k_l in lean furnace tests with water vapor [2, 11].

A strong temperature dependence of SiC recession due to SiO_2 volatility was produced in synthetic rich gas mixtures, as shown in the composite TGA curves of Fig. 3. Here very little volatility could be detected below 1350°C using the same paralinear model and data analysis [4]. However, at 1400°C and above, the volatility rates were appreciable.

A comparison of the SiC weight loss rates in lean and rich furnace test environments is shown in the Arrhenius plot of Fig. 4. A higher temperature dependency is observed for rich environments. It should be noted that the fuel-rich tests were performed at 1/10 the gas flow of the fuel-lean exposures. Also, X-ray diffraction and SEM confirmed that a continuous cristobalite scale was indeed present under all furnace exposures and that active oxidation was not responsible for these weight losses.

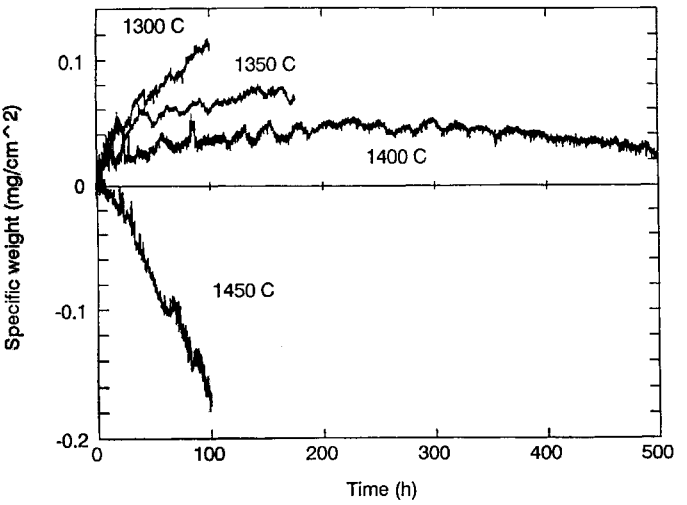

Figure 3. Temperature dependence of the weight change behavior of CVD SiC in synthetic rich TGA furnace environments ($4\%H_2-12\%H_2O-10\%CO-7\%CO_2-N_2$).

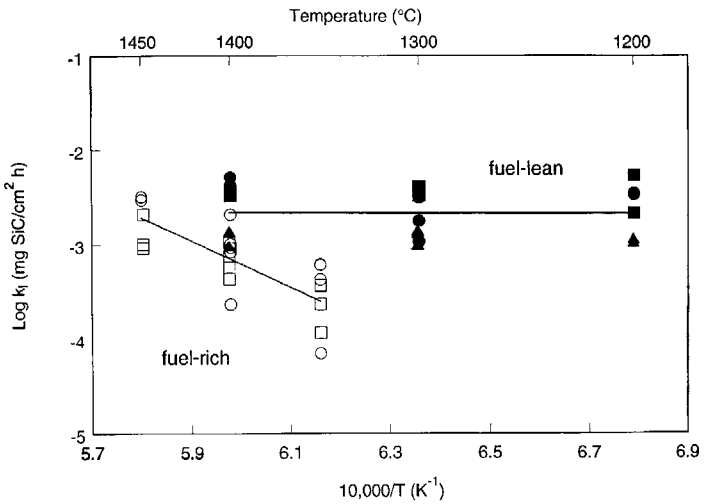

Figure 4. Comparative Arrhenius plots of SiC loss rates for synthetic lean (filled symbols) and rich (open symbols) TGA furnace environments. (Circles = CVD SiC; squares = pre-oxidized SiC; triangles = fused quartz.)

3.2. Burner rig tests

In HPBR testing, linear weight loss rates were also observed, although the initial interval of weight gains characteristic of paralinear oxidation were generally not observable. A selection of test results is shown in Fig. 5 for CVD SiC tested under fuel-lean conditions. Linear rates of thickness loss also occurred and showed similar temperature dependencies [8]. The correlation between SiC thickness and weight loss, calculated from the density of SiC (3.2 g/cm^3), is 3.1 μm for each mg/cm^2

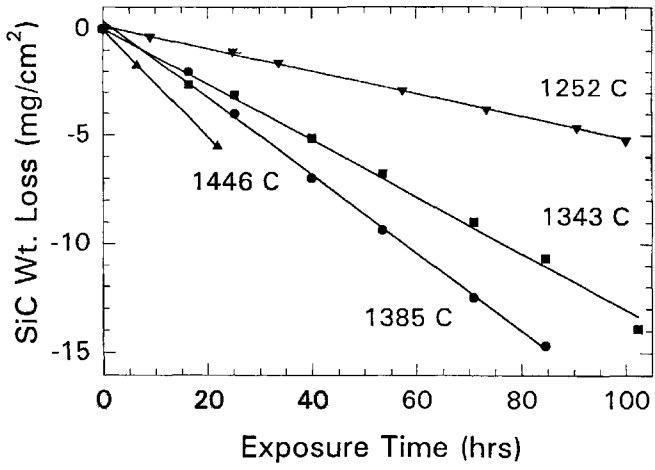

Figure 5. The effect of sample temperature on the linear rate of SiC weight loss under fuel-rich HPBR combustion conditions ($P = 6$ atm, $v = 18$–20 m/s).

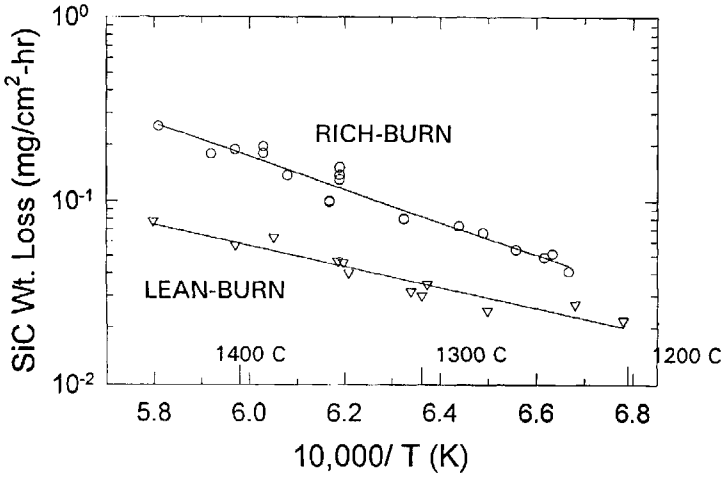

Figure 6. Comparative Arrhenius plots of SiC recession rates under fuel-rich and fuel-lean HPBR combustion ($P = 6$ atm, $v = 18$–23 m/s).

of SiC consumed. In close agreement, a factor of 2.9 was measured experimentally, indicating that weight loss is also a reliable indicator of surface recession.

Over 30 test runs at 6 atm yielded the two corresponding Arrhenius curves in Fig. 6. A somewhat higher absolute recession rate and activation energy is indicated for rich combustion compared to lean. Sintered SiC (Hexoloy) and number of composite samples (DuPont SiC/SiC, enhanced SiC/SiC, Supertemp, and RT 42 coatings) all showed weight loss behavior basically equivalent to that of CVD SiC under the same range of test conditions.

Similar experiments were performed on CVD and sintered (AS 800) Si_3N_4 under fuel-lean conditions. The weight change curves in Fig. 7 show immediate linear

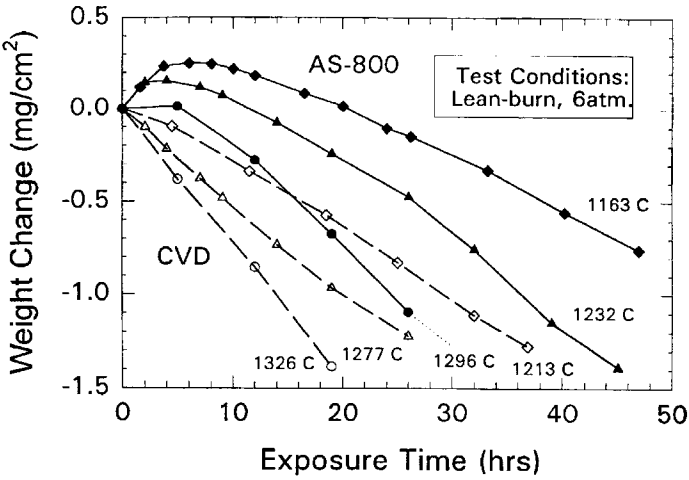

Figure 7. Linear and paralinear oxidation curves for CVD and sintered (AS 800) Si_3N_4 under lean-burn combustion conditions ($P = 6$ atm).

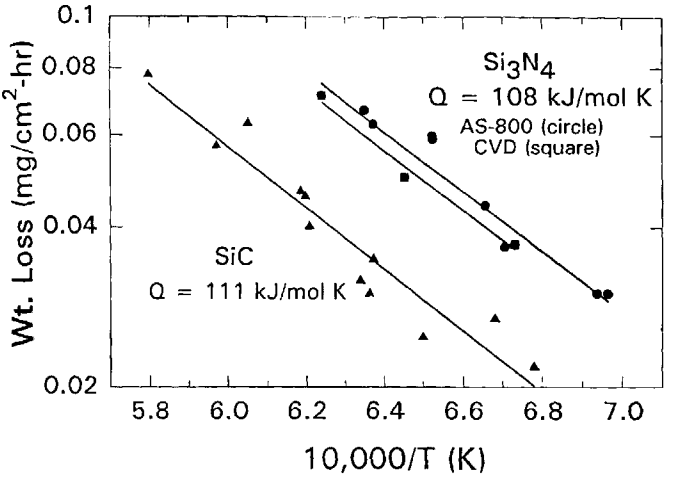

Figure 8. Comparative Arrhenius plots of SiC and Si_3N_4 lean-burn recession rates.

loss rates for the CVD material, but paralinear behavior for the sintered Si_3N_4. Paralinear behavior has been reported for furnace tests of SiC and Si_3N_4 in water vapor [2, 10, 11], i.e. initial weight gains before approaching a linear weight loss rate. The temperature dependency of Si_3N_4 recession rates show activation energies similar to those for SiC in the Arrhenius plot of Fig. 8. However the absolute value of the rate is 1.8 times that of SiC. In synthetic ($50\%H_2O/O_2$) fuel-lean furnace TGA tests, the same materials exhibited volatility rates nearly equal to those of SiC [10]. At this time there is no plausible explanation for these differences.

Another series of tests determined that increased pressure resulted in increased volatility rates [8]. However, an absolute relationship can not be directly claimed

because of the simulteneous decrease in velocity. Pressure effects will therefore be discussed after the general volatility model is presented.

4. DISCUSSION

4.1. Volatility rate model

The general temperature dependence is derived from the equilibrium constants of the pertinent reactions:

$$\Delta G_0 = -RT \ln K_{\text{eq.}}. \tag{1}$$

For example, the reaction of SiO_2 ($a = 1$) with water vapor has an equilibrium vapor pressure of $Si(OH)_4$ given by:

$$SiO_2 + 2H_2O\ (g) = Si(OH)_4\ (g), \tag{2}$$

$$K_{\text{eq.}} = \frac{P_{Si(OH)_4}}{a_{SiO_2} * P_{H_2O}^2}, \tag{3}$$

$$P_{Si(OH)_4} = \exp\left(-\frac{\Delta G_0}{RT}\right) * P_{H_2O}^2, \tag{4}$$

or for a possible rich-burn reaction:

$$SiO_2 + H_2\ (g) = SiO\ (g) + H_2O\ (g), \tag{5}$$

$$K_{\text{eq.}} = \frac{P_{SiO} * P_{H_2O}}{a_{SiO_2} * P_{H_2}}, \tag{6}$$

$$P_{SiO} = \exp\left(-\frac{\Delta G_0}{RT}\right) * \frac{P_{H_2}}{P_{H_2O}}. \tag{7}$$

A model of SiO_2 volatilization was developed in detail in [2, 9] and is illustrated in the schematic of Fig. 9. In short, material removal was approximated by diffusion of a volatile species (shaded spheres) through a boundary layer moving with laminar flow across the reactant surface. Ideally, velocity varies across the boundary layer from zero at the sample surface to the free stream velocity at the boundary edge (vectors). The equation describing such a flux is given by the following relationship as described in [2]:

$$J = 0.664(Re)^{1/2}(Sc)^{1/3}\frac{D\rho v}{L}, \tag{8}$$

where Re = Reynolds number and Sc = Schmidt number. Or, equivalently:

$$J = 0.664\left(\frac{\rho' vL}{h}\right)^{1/2}\left(\frac{h}{\rho' D}\right)^{1/3}\frac{D\rho}{L}, \tag{8a}$$

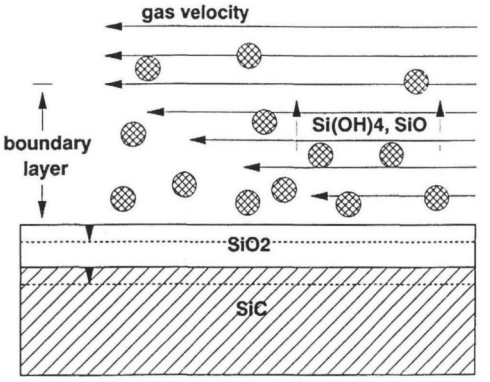

Figure 9. Schematic of physical SiO_2 scale volatility process (gaseous diffusion through a moving boundary layer) and corresponding SiC recession.

where v is the linear gas velocity, h is the gas viscosity, D is the interdiffusion coefficient for the volatile species in the major combustion gas component, ρ is the concentration of the volatile species at the solid-gas interface, ρ' is the concentration of the major gas component, and L is the characteristic sample length parallel to the flow and over which the volatility is averaged. Other details required for the calculation are described in [2, 9]; the objective here is to illustrate the origins of the terms needed for a simple functional relationship between recession rate and temperature, pressure, and velocity.

The net result of the factors in equations (4), (7), and (8) on the flux of $Si(OH)_4$ and SiO volatile products is given by equations (9) and (10), respectively.

$$J_{Si(OH)_4} \propto \left\{ \exp\left(-\frac{\Delta G_0}{RT} \right) \right\} v^{1/2} \frac{P_{H_2O}^2}{P_{total}^{1/2}}, \tag{9}$$

$$J_{SiO} \propto \left\{ \exp\left(-\frac{\Delta G_0}{RT} \right) \right\} v^{1/2} \frac{P_{H_2}}{P_{H_2O} * P_{total}^{1/2}}. \tag{10}$$

Given that the pressure of the reactants varies directly with the total system pressure, the functional forms can be further simplified:

$$J_{Si(OH)_4} \propto \left\{ \exp\left(-\frac{\Delta G_0}{RT} \right) \right\} v^{1/2} \left(P_{total}^{3/2} \right), \tag{9a}$$

$$J_{SiO} \propto \left\{ \exp\left(-\frac{\Delta G_0}{RT} \right) \right\} v^{1/2} \left(P_{total}^{-1/2} \right). \tag{10a}$$

4.2. Comparison with measured data

A general parametric dependency according to $\{\exp(-Q/RT)\}(P^x v^y)$ can thus be expected for recession rates. From the appropriate thermodynamics and flow conditions, the vapor species flux was calculated for low velocity, 1 atm furnace and high velocity, 6 atm burner rig conditions and compared to the experimental data, Figs 10 and 11. For lean exposures it is seen that good agreement exists for the measured and calculated values, assuming an $Si(OH)_4$ gaseous reaction product, Fig. 10.

For rich conditions, good agreement is found for the furnace exposures, assuming an SiO vapor species, Fig. 11. However, the higher pressures of the burner rig test render the predicted vapor pressure and contribution of this species to be minor. The potential contribution of the $Si(OH)_4$ species is shown, but the lack of agreement

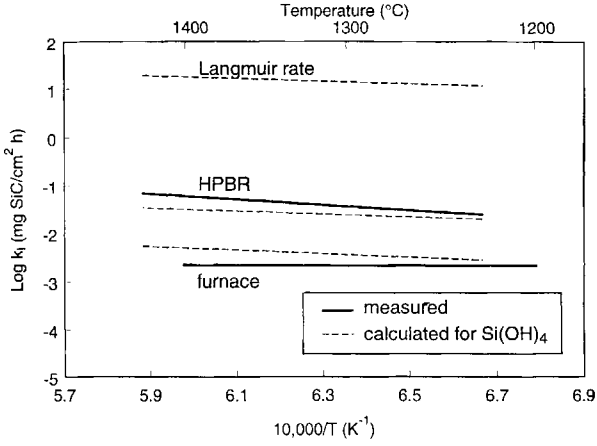

Figure 10. Comparison of calculated and measured SiC recession rates under lean conditions.

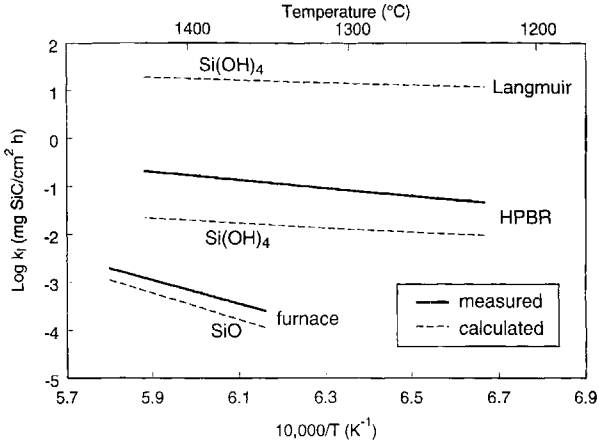

Figure 11. Comparison of calculated and measured SiC recession rates under rich conditions.

suggests that other species may be controlling. While $SiO(OH)_2$ and $Si_2(OH)_6$ molecules have been considered, the available thermodynamic data does yet not support any single species [9].

The Langmuir rates are also shown in these figures as an upper bound to what would be predicted if there were no gaseous boundary layer diffusion control or what would be approached as the flow exceeded turbulent conditions:

$$J_{\text{Langmuir}} = P_{\text{species}}\left(\frac{M_{\text{species}}}{2\pi RT}\right)^{1/2}, \tag{11}$$

where P is the equilibrium vapor pressure and M is the molecular weight of the volatile species. The Langmuir rates are at least two orders of magnitude greater than those produced by HPBR exposures. Thus the volatility rates measured in burner rig tests more nearly approach those calculated from the boundary layer equation, even though ideal laminar flow is not expected in these tests.

4.3. Normalized recession rates

A second series of HPBR experiments was performed to illustrate the effects of pressure and velocity. These had the two-fold purpose of verifying the diffusional model as well as providing key information (Q and x) regarding the controlling chemical mechanism. Velocity and pressure were interdependent variables in the high pressure burner rig, therefore the data was displayed according to a combined variable, i.e. normalized with respect to a $P^{3/2}v^{1/2}$ term, Fig. 12. The results show that both rich and lean exposures produce recession rates that conform reasonably well to a boundary layer diffusion model with a $P^{3/2}$ pressure dependency, where

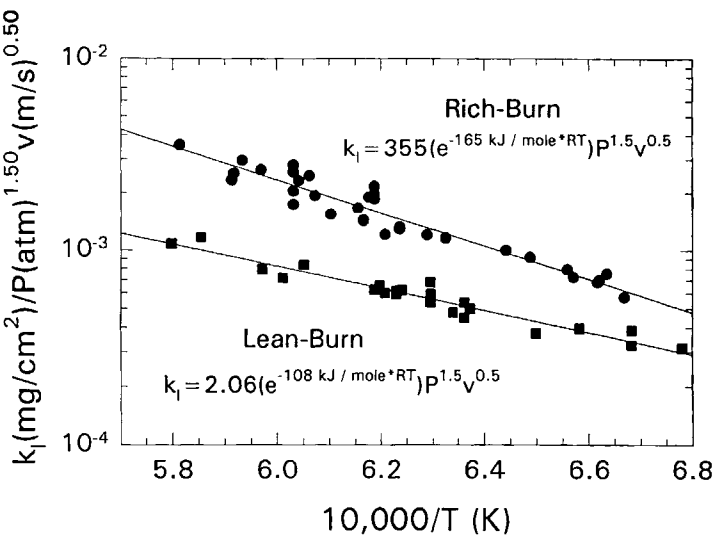

Figure 12. Universal SiC recession rates in HPBR tests, normalized for all pressures and velocities by the factor $P^{3/2}v^{1/2}$.

Table 1.
Projected SiC recession (μm per 1000 h) for various temperatures under generic combustor conditions

Temp. (°C)	Lean-burn (10 atm, 90 m/s)	Rich-burn (10 atm, 30 m/s)
1000	70	40
1100	140	130
1200	270	330
1300	480	760
1400	790	1580
1500	1230	3010

again the rich burn rates and activation energy were higher. More precisely, multiple linear regression analysis of lean and rich data sets, containing 24 and 34 points, respectively, yielded the following fits to the data [8]:

$$\text{lean:} \quad k_l\ (\text{mg/cm}^2) = 2.04 \exp(-108\ \text{kJ/mol}/RT) P^{1.50} v^{0.50}, \quad R^2 = 0.98, \tag{12}$$

$$\text{rich:} \quad k_l\ (\text{mg/cm}^2) = 82.5 \exp(-159\ \text{kJ/mol}/RT) P^{1.74} v^{0.69}, \quad R^2 = 0.95, \tag{13}$$

where pressure is in atmospheres, velocity in meters/second and temperature in K.

The lean relationship is thus in exceptional agreement with the predicted $P^{3/2}v^{1/2}$ boundary layer analysis, which includes the pressure dependency for the $Si(OH)_4$ molecule. The rich relationship is less clear, giving a pressure dependency somewhat higher than 1.5 and a non-ideal velocity exponent. In any event, these empirical equations can be used to predict recession under any variety of conditions. Examples of lean and rich-burn recession under some typical combustor conditions are shown in Table 1. Clearly, high values are obtained at temperatures equal to and above 1200°C. High rates would also be expected for turbine airfoils because of the higher pressures and velocities associated with this stage.

5. CONCLUSIONS

The oxidation behavior of CVD and sintered SiC and Si_3N_4 materials was evaluated under synthetic (TGA furnaces) and actual (HPBR) fuel-rich and fuel-lean combustor conditions. All tests have produced weight loss rates indicative of gaseous reaction products for all materials. The furnace tests produced rates that agreed with model calculations based on $Si(OH)_4$ (fuel-lean) or SiO (fuel-rich) volatile species. The high pressure burner rig tests produced pressure and velocity dependencies which also suggest volatilization phenomena. Good regression fits to the recession rates were obtained for the functional form: $A^*\{\exp(-Q/RT)\}P^x v^y$. Recession is seen to be higher under fuel-rich HPBR conditions than under fuel-lean;

but both will result in significant recession after long term exposures. The critical fuel-lean species appears to be $Si(OH)_4$ under furnace and burner rig conditions, but is known to be SiO only for the fuel-rich furnace (atmospheric) condition. Si_3N_4 materials also exhibited scale volatility in fuel-lean furnace and HPBR conditions.

REFERENCES

1. N. S. Jacobson, High temperature durability considerations for HSCT combustor, NASA Tech. Paper 3162 (January, 1992).
2. E. J. Opila and R. E. Hann, Paralinear oxidation of CVD SiC in water vapor, *J. Am. Ceram. Soc.* **80** (1), 197–205 (1997).
3. E. J. Opila, D. S. Fox and N. S. Jacobson, Mass spectrometric identification of Si-O-H (g) species from the reaction of silica with water vapor at atmospheric pressure, *J. Am. Ceram. Soc.* **80** (4), 1009–1012 (1997).
4. D. S. Fox, E. J. Opila and R. E. Hann, Paralinear oxidation of CVD SiC in a simulated rich-burn environment, submitted to the *J. Am. Ceram. Soc.*
5. J. L. Schienle, Durability testing of commercial ceramic materials, NASA CR-198497 (January, 1996).
6. Y. Etori *et al.*, Oxidation behavior of ceramics for gas turbines in combustion gas flow at 1500°C, ASME Paper 97-GT-355 (June, 1997).
7. R. C. Robinson, SiC recession due to SiO_2 scale volatility under combustor conditions, NASA CR-202331 (March, 1997).
8. R. C. Robinson and J. L. Smialek, SiC recession due to SiO_2 scale volatility under combustor conditions. Part I: Experimental results and empirical model, *J. Am. Ceram. Soc.* (in press).
9. E. J. Opila, J. L. Smialek, R. C. Robinson, D. S. Fox and N. S. Jacobson, SiC recession due to SiO_2 scale volatility under combustor conditions. Part II: Thermodynamics and gaseous diffusion model, *J. Am. Ceram. Soc.* (in press).
10. D. S. Fox, E. J. Opila and Q. N. Nguyen, Paralinear oxidation of silicon nitride in a water vapor/oxygen environment, in: *HTMX IX Proceedings*, Penn State (1997).
11. E. J. Opila, The variation of the oxidation rate of SiC with water vapor pressure, *J. Am. Ceram. Soc.* (in press).